

# Screening effects in Coulomb frustrated phase separation

C. Ortix,<sup>1</sup> J. Lorenzana,<sup>2,3</sup> M. Beccaria,<sup>1</sup> and C. Di Castro<sup>2</sup>

<sup>1</sup>*Dipartimento di Fisica, Università del Salento and INFN Sezione di Lecce, Via per Arnesano, 73100 Lecce, Italy.*

<sup>2</sup>*SMC-Istituto Nazionale di Fisica della Materia and Dipartimento di Fisica,*

*Università di Roma “La Sapienza”, P. Aldo Moro 2, 00185 Roma, Italy.*

<sup>3</sup>*ISC-Consiglio Nazionale delle Ricerche, Via dei Taurini 19, 00185 Roma, Italy.*

(Dated: September 13, 2018)

We solve a model of phase separation among two competing phases frustrated by the long-range Coulomb interaction in two and three dimensions (2D / 3D) taking into account finite compressibility effects. In the limit of strong frustration in 2D, we recover the results of R. Jamei, S. Kivelson, and B. Spivak, Phys. Rev. Lett. **94**, 056805 (2005) and the system always breaks into domains in a narrow range of densities, no matter how big is the frustration. For weak frustration in 2D and for arbitrary frustration in 3D the finite compressibility of the phases is shown to play a fundamental role. Our results clarify the different role of screening in 2D and 3D systems. We discuss the thermodynamic stability of the system near the transition to the phase separated state and the possibility to observe it in real systems.

PACS numbers: 71.10.Hf, 64.75.+g, 71.10.Ca

## I. INTRODUCTION

In the presence of long-range forces the tendency towards phase separation among two competing phases may lead to self-stabilized domain patterns of finite size<sup>1,2,3,4,5</sup>. A prominent example is provided by charged systems compensated by a rigid background. The Coulomb energy cost grows faster than the size of the system and precludes macroscopic phase separation. Therefore one finds either uniform phases or phases with domains of one phase hosted by the other one<sup>2,3,6,7,8,9,10,11,12,13,14</sup>. In the mixed state the finite Coulomb energy arising from the mismatch between the local electronic charge  $-en_i$  and the fixed background charge  $e\bar{n}$ , competes with the surface energy to determine the typical size of the domains.

Experiments in layered materials like cuprates<sup>15,16,17</sup>, ruthanates<sup>18</sup>, manganite thin films<sup>19</sup> and in the two-dimensional electron gas<sup>20,21</sup> have fueled interest in the two-dimensional version of this problem<sup>13,14,22</sup>. In particular the recent discovery of pronounced anisotropies in transport properties<sup>18,20</sup> are consistent with the proposal of exotic electronic liquid phases<sup>23</sup> analogous to the intermediate order states of liquid crystals<sup>24</sup>.

Jamei, Kivelson and Spivak<sup>13</sup> have analyzed a model in which the energies of two infinitely compressible uniform phases cross each other at a certain density  $n_c$ . They have shown that in 2D, sufficiently close to  $n_c$ , the system always breaks into domains for any level of frustration due to the long-range Coulomb (LRC) interaction. They have focused on the universal aspects arising for large frustration where the compressibility turns out to be negligible. On the other hand it has been argued that screening, driven by finite compressibility, plays a fundamental role on Coulomb frustrated phase separation<sup>9,14</sup>. It is thus of interest to analyze its effect for the full range of frustration and, in this respect, to clarify the difference between the two-dimensional (2D) and three-dimensional

(3D) case.

In this work we solve a model of Coulomb frustrated phase separation, similar to the one of Ref. 13 but augmented to take into account the finite compressibility of the phases (Sec. II). This allows us to derive the phase diagram in 2D from the limit of strong frustration down to the limit of zero frustration where phase separation is determined by Maxwell construction (MC) and the compressibility of the phases, by sure, cannot be neglected. The interplay between the screening and the size of inhomogeneities is discussed in two-dimensional systems (Sec. III) and three-dimensional systems (Sec. IV). Both cases are compared at the end of Sec. IV. We show that for not so large frustration in 2D and practically everywhere in 3D the physics of the mixed state can be captured in a simple approximation where the density variation inside the inhomogeneities is neglected. We argue that the strongly frustrated 2D mixed state regime is experimentally hardly accessible and characterized by a large negative electronic compressibility that can lead to a volume collapse of the lattice. The model presented here can be solved exactly and confirms the conclusions of previous approximated treatments. In particular it illustrates the general rule found in Refs. 9,11 that for generic value of the parameters inhomogeneities can not have all linear dimensions larger than the 3D screening length.

## II. MODEL AND GENERAL SOLUTION

We consider a ferromagnetic Ising model linearly coupled to a charged fluid as a generic model of a first order density driven phase transition with Coulomb interac-

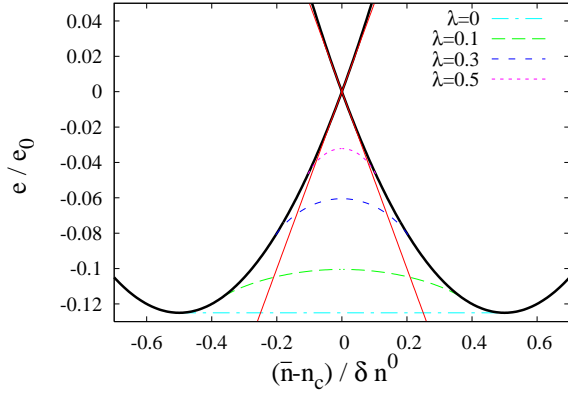


FIG. 1: (Color online) Behavior of the free energy density for the uniform phases with  $s = \pm 1$  in the present model (thick lines) compared with the  $\kappa \rightarrow \infty$  model discussed in Ref.13 (thin full lines). The dashed lines are the energy density of the mixed state solutions in 2D systems for different values of the frustrating parameter defined in Sec. III. The energy density is measured in unit of the characteristic phase separation energy gain  $e_0 \equiv (\delta n^0)^2/\kappa = 2\pi Q^2(\delta n^0)^2 l_s$ . The dot-dashed line corresponds to the Maxwell construction ( $\lambda = 0$ ).

tions. The Hamiltonian reads:

$$\mathcal{H} = -J \sum_{\langle ij \rangle} s_i s_j - \frac{\Delta \mu_c}{2} \sum_i s_i (n_i - n_c) + \frac{1}{2\kappa} \sum_i (n_i - n_c)^2 + \frac{Q^2}{2} \sum_{ij} (n_i - \bar{n}) \frac{1}{r_{ij}} (n_j - \bar{n}) \quad (1)$$

where  $s_i = \pm 1$ , the index  $i$  runs over the sites of a hypercubic lattice of dimension  $D = 2, 3$  and  $\bar{n}$  is the average charge. Instead of the present Ising term one could consider, as in Ref. 13 a double-well potential in the very large barrier limit. In solid state systems the strength of the Coulomb interaction will be given by  $Q^2 = e^2/\epsilon_0$  with  $\epsilon_0$  the static dielectric constant of the environment (*i.e.* excluding the mobile electrons).

For the two uniform phases ( $n_i = \bar{n}$ ), the energy as a function of density consists of two parabolas that cross at  $n_c$  with chemical potential difference  $\Delta \mu_c$ , minima at  $\bar{n} = n_c \pm \delta n^0/2$  and  $\delta n^0 \equiv \kappa \Delta \mu_c$  as illustrated by the thick lines in Fig. 1. For  $Q = 0$ , according to the ordinary Maxwell construction, the system phase separates when the average density  $\bar{n}$  is in a window of width  $\delta n^0$  around the crossing density. The energy of this solution is depicted with the dot-dashed horizontal line in Fig. 1.

We are assuming that the two uniform phases have the same compressibility to make the problem solvable. A related model in 3D has been considered in Ref. 9. The 2D case in which one of the phases is incompressible has been analyzed in Ref. 14, whereas Ref. 13 corresponds to the case in which both phases are infinitely compressible and Maxwell construction is not defined ( $\kappa \rightarrow \infty$ , thin full lines in Fig. 1).

Interfaces of the Ising order parameter are sharp

by construction with a surface tension given by  $\sigma = 2J/a^{D-1}$  where  $a$  is the lattice constant. The linear term in  $\Delta \mu_c$  expresses that the homogeneous phase with  $s_i = 1$  ( $\uparrow$ ) is favored at higher densities, and the phase with  $s_i = -1$  ( $\downarrow$ ) at lower densities.

We solve the problem in the limit in which domains are much larger than the lattice constant and replace the site index by a continuum variable, *i.e.*  $s(\mathbf{r})$ ,  $n(\mathbf{r})$  in a volume  $V$ . Hereafter we take  $a \equiv 1$ . For each mixed state, the geometry of the domains defines  $s(\mathbf{r})$  and its Fourier transform  $s(\mathbf{q})$ . Writing the energy in the Fourier space, the  $\mathbf{q} = 0$  component of the Coulomb term is canceled. At  $\mathbf{q} \neq 0$ , upon minimizing with respect to the charge distribution, one gets:

$$n(\mathbf{q}) (\kappa^{-1} + 2^{D-1} \pi Q^2 / |\mathbf{q}|^{D-1}) = \frac{\Delta \mu_c}{2} s(\mathbf{q}) \quad (2)$$

This equation has a simple physical interpretation by noticing that for a fixed domain configuration

$$\mu(\mathbf{r}) \equiv -\frac{\Delta \mu_c}{2} s(\mathbf{r}) + \kappa^{-1} [n(\mathbf{r}) - n_c]$$

represents the local chemical potential and the electrostatic potential can be put as:

$$v(\mathbf{r}) = \int d\mathbf{r}' \phi(\mathbf{r} - \mathbf{r}') n(\mathbf{r}').$$

Here  $\phi(\mathbf{r})$  is the Fourier transform of

$$\phi(\mathbf{q}) \equiv 2^{D-1} \pi Q^2 / |\mathbf{q}|^{D-1},$$

as follows from Poisson equation in three and two-dimensional systems<sup>14</sup> in the presence of the 3D Coulomb interaction and plays the role of the “effective” Coulomb interaction. With these definitions Eq. (2) states that the total local electrochemical potential  $\mu(\mathbf{r}) + v(\mathbf{r})$  is constant. The latter condition is the generalization to electronic systems of the Maxwell condition for neutral fluids that is enforced by the constancy of the local chemical potential across different phases.

We can now use Eq. (2) to eliminate the charge from the energy and obtain an energy functional that depends only upon  $s(\mathbf{q})$ :

$$E = \sigma \Sigma - \frac{\Delta \mu_c}{2} s_0 (\bar{n} - n_c) + \frac{V}{2\kappa} (\bar{n} - n_c)^2 + \frac{\Delta \mu_c^2}{8V} \sum_{\mathbf{q} \neq 0} \frac{s_{\mathbf{q}} s_{-\mathbf{q}}}{[\kappa^{-1} + 2^{D-1} \pi Q^2 / |\mathbf{q}|^{D-1}]} \quad (3)$$

where we have dropped an irrelevant constant. The first term in Eq. (3) is the surface energy of the sharp interfaces with  $\Sigma$  indicating the total surface of the interfaces. The second and third terms are the  $\mathbf{q} = 0$  contribution from the bulk free energy of the competing phases. The last term comes from the  $\mathbf{q} \neq 0$  contribution of the last three terms of Eq. (1) after eliminating the charge via Eq. (2).

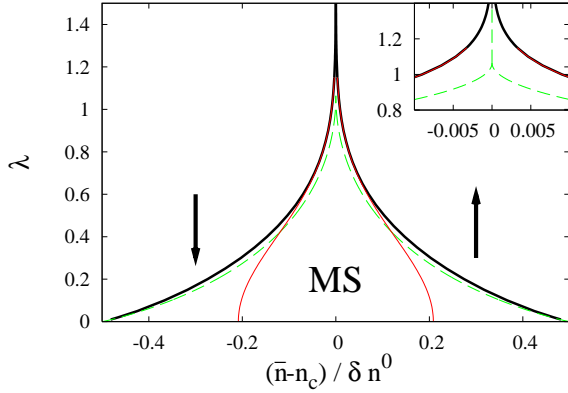


FIG. 2: (Color online) The phase diagram for the smectic stripe solution in 2D. The central region corresponds to the mixed state (MS). The thick line is the exact solution of the present model with finite compressibility, the thin full line is the  $\kappa \rightarrow \infty$  limit taking the short distance cutoff of Ref. 13 equal to the present screening length  $l_s$ . The dashed line is the UDA. The inset shows an enlargement near the crossing density  $n_c$  where the UDA predicts a critical value of the frustrating parameter.

Eq. (3) has to be optimized with respect to the geometry of the domains. Here we restrict to a periodic structure of alternating  $s = \pm 1$  stripes. This state can be interpreted as a *smectic* electronic liquid phase that possesses orientational order and breaks the translational symmetry only in one direction. Possibly, fluctuations of the stripe order can restore the translational symmetry<sup>25</sup> thus leading to a *nematic* phase. For the smectic stripe state the problem can be solved analytically (Secs. III,IV). Other states with different geometries like circular drops can be treated numerically and will not be considered in this work.

### III. 2D SYSTEMS

In this section we consider 2D systems. From Eq. (3) the energy density ( $e \equiv E/V$ ) of a mixed state with alternating  $s = 1$  stripes of width  $2R_d$  and  $s = -1$  stripes of width  $2(R_c - R_d)$ , can be cast as:

$$e = \frac{\sigma}{R_c} + \Delta\mu_c \left( \frac{1}{2} - \nu \right) (\bar{n} - n_c) + \frac{(\bar{n} - n_c)^2}{2\kappa} - \frac{\Delta\mu_c^2}{2^{D-1}\pi Q^2(2R_c)} \left[ u \left( 0, \frac{R_c}{l_s} \right) - u \left( 2\nu, \frac{R_c}{l_s} \right) \right] \quad (4)$$

where we introduced the two-dimensional screening length

$$l_s \equiv (2\pi Q^2 \kappa)^{-1},$$

and the volume fraction  $\nu \equiv R_d/R_c$  of the  $s = 1$  phase. We also define the Fourier transform of the effective in-

teraction  $u_q$ :

$$u \left( \frac{x}{R_c}, \frac{R_c}{l_s} \right) \equiv \frac{1}{2R_c} \sum_{n \neq 0} e^{i q_n x} u_{q_n} \quad q_n \equiv \frac{\pi n}{R_c}$$

with  $n$  running over nonzero integers and

$$u_q \equiv \frac{1}{|q|(1 + l_s|q|)}.$$

This effective interaction coincides in this case with the effective 3D screened Coulomb interaction in two-dimensional electronic systems discussed in Refs. 26 and 14.

Eq. (4) can be recast in dimensionless form measuring the energy in units of the characteristic phase separation energy density gain  $e_0 \equiv (\delta n^0)^2/\kappa$ , lengths in units of  $l_s$  and densities in units of  $\delta n^0$ :

$$\frac{e}{e_0} = \lambda^2 \frac{l_s}{2R_c} + \left( \frac{1}{2} - \nu \right) \left( \frac{\bar{n} - n_c}{\delta n^0} \right) + \frac{1}{2} \left( \frac{\bar{n} - n_c}{\delta n^0} \right)^2 - \frac{l_s}{2R_c} \left[ u \left( 0, \frac{R_c}{l_s} \right) - u \left( 2\nu, \frac{R_c}{l_s} \right) \right] \quad (5)$$

Here we defined a dimensionless coupling:

$$\lambda^2 \equiv 4\pi\sigma Q^2/\Delta\mu_c^2$$

that parametrizes the mixed state energy density. Apart from numerical constants,  $\lambda$  coincides with the frustrating parameter defined in Refs. 9,14 that measures the strength of the frustration due to LRC interaction and surface energy with respect to  $e_0$ .

The dimensionless free energy density, Eq. (5), depends upon  $\lambda$ ,  $(\bar{n} - n_c)/\delta n^0$ ,  $\nu$  and  $R_c/l_s$ . Minimizing with respect to the volume fraction  $\nu$  and  $R_c/l_s$  we obtain the phase diagram in the  $\lambda$ -density plane shown in Fig. 2 with the thick lines.

As in many other situations, increasing the frustration, the region of stability of the uniform phases is increased. As for the  $\kappa = \infty$  case (thin full line in Fig. 2), there is no direct first-order transition between the two homogeneous phases no matter how big is  $\lambda^{13}$ . Indeed the transition line is logarithmically singular at  $\bar{n} = n_c$  and thus for large  $\lambda$  the mixed state is enclosed in the exponentially narrow range

$$|\bar{n} - n_c| < \delta n^0 e^{-\pi\lambda^2}. \quad (6)$$

Clearly, observation of the mixed state for large  $\lambda$  requires an enormously accurate control of the density  $\bar{n}$  which may be hard to achieve in practice. As frustration decreases, the range of densities of the mixed state grows and converges to the Maxwell construction range when  $\lambda \rightarrow 0$ .

Close to the divergence, the present phase diagram coincides with the one for infinite compressibility (thin full line in Fig. 2) provided one takes the short-distance cutoff of Ref. 13 equal to  $l_s$ . This agreement is due to the

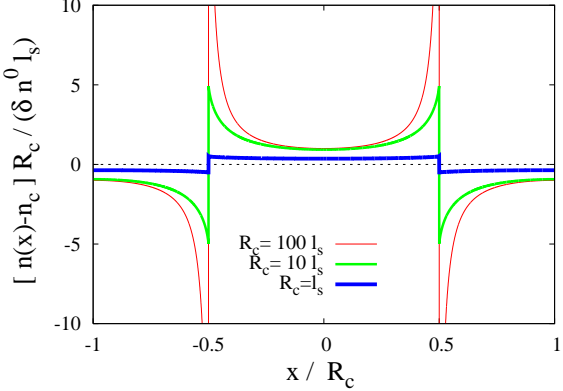


FIG. 3: (Color online) Charge density modulation for a cut perpendicular to a stripe in 2D at  $\bar{n} = n_c$ ,  $R_d = R_c/2$  and three different values of the screening length corresponding to  $\lambda \sim 0.2$  ( $R_c = l_s$ ),  $\lambda \sim 0.7$  ( $R_c = 10l_s$ ) and  $\lambda \sim 1.1$  ( $R_c = 100l_s$ ). In the case  $R_c/l_s \rightarrow \infty$  the charge density diverges at the boundary. A finite  $l_s$  removes the divergence.

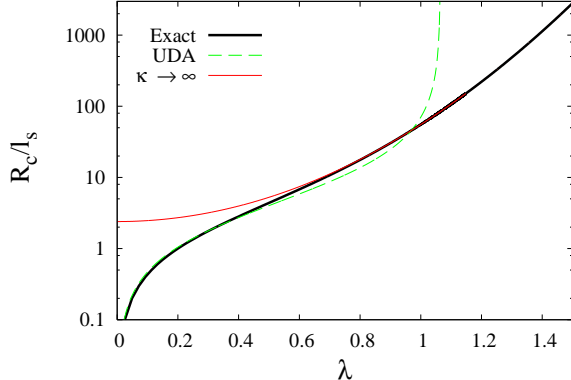


FIG. 4: (Color online) Behavior of  $R_d$  (log scale) at the crossing density as a function of the frustrating parameter. The thick line is the solution of the present model while the thin line is the infinite compressibility limit<sup>13</sup>. The UDA is the dashed line.

fact that in the highly frustrated regime the physics is determined by the slow power-law relaxation of the charge (Fig. 3) far from the stripe boundary. In fact the stripe width is much larger than the screening length and indeed behaves as (c.f. Fig. 4)

$$R_d = \frac{R_c}{2} \sim l_s e^{\pi \lambda^2} \quad (7)$$

whereas the finite compressibility of the present model affects the charge only in a range of order  $l_s$  from the boundary. Its effect is to remove the unphysical divergence of the charge density at the stripe boundary arising when  $l_s = 0$  (Fig. 3). On the contrary, for low  $\lambda$  the stripe size is of the order of the screening length  $R_d \sim l_s \lambda$  (Fig. 4) and the finite compressibility is relevant.

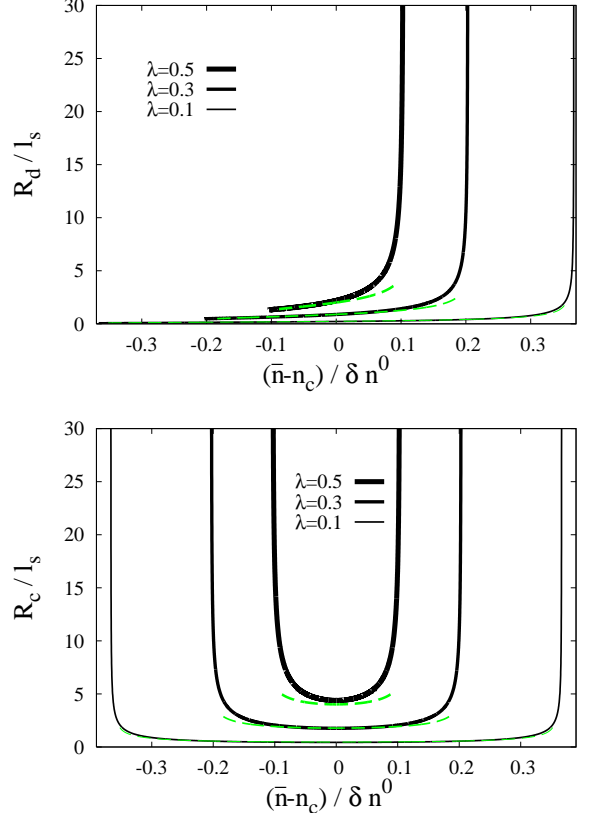


FIG. 5: (Color online) Behavior of the width (top panel) and periodicity (bottom panel) of  $\uparrow$  stripes in 2D systems for different values of  $\lambda < 1$ . The dashed lines correspond to the uniform density approximation whereas the full line is the exact solution. Notice that the  $\uparrow$  stripes are the minority phase for  $n < n_c$  and the majority phase for  $n > n_c$ .

For practical applications and for more complicated forms of the energy specifying the homogeneous phases, it may be convenient to use a uniform density approximation (UDA) in which one neglects the spatial variation of the density inside each inhomogeneity<sup>9,14</sup>. The phase diagram in this case is also plotted in Fig. 2 with a dashed line. As in Ref.14 the electrostatic energy has been approximated by taking into account only the self interaction *i.e.* we neglect the Coulomb interaction among different stripes.

Remarkably the UDA with this crude approximation for the Coulomb interaction gives very accurate results in a wide range of the phase diagram except around the crossing density, since it misses the logarithmic singularity and then predicts a critical value  $\lambda_c$  of the frustrating parameter above which the uniform phases would be stable as in the 3D case<sup>9</sup> and a first order phase transition among them would occur (see the inset of Fig. 2). Approaching  $\lambda_c$  from below, the MS disappears with a divergent stripe size (see Fig. 4) in contrast with the exact results where the MS persists with a finite stripe size.

For  $\lambda < \lambda_c$ , at the onset of the mixed state the UDA

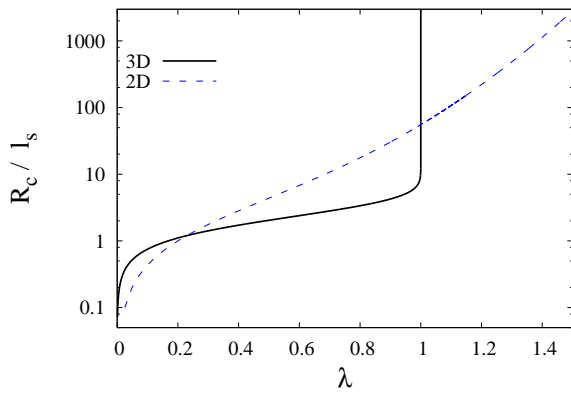


FIG. 6: (Color online) Behavior of the period of layers (log scale) vs  $\lambda$  at the crossing density in 3D (thick line) and 2D systems (dashed line).

predicts a first-order transition with the minority phase stripe size and the stripe periodicity that stay finite (see Fig. 5). Taking into account the local dependence of the electronic density, the jump in the periodicity of the stripes at the transition is substituted by a square root divergence. Thus the uniform-mixed state transition is characterized by a finite value of the minority phase stripe size and a divergent periodicity which corresponds to a second-order transition<sup>27</sup>. Apart from the singularity at the transition between the uniform phase and the smectic stripe phase, the behavior of the mixed state for not so large frustration is very well represented by the UDA (Fig. 4, 5).

For  $\lambda > \lambda_c$  relaxation of the UDA produces the logarithmic singularity which, as stated above, affects in an exponentially narrow region the phase diagram. Furthermore, according to Eq. (7), for large  $\lambda$  the size of the domains can quickly reach the size  $L$  of the system. Finite  $L$  will introduce a cutoff to the singularity

$$\lambda_c^* \sim [(\log L/l_s)/\pi]^{1/2}.$$

For  $\lambda > \lambda_c^*$  the transition will look first order like.

For  $\lambda < \lambda_c^*$  the transition is second order like, however the effect of the mixed state solution is to produce an exponentially small rounding of the singularities in thermodynamic quantities quite hard to distinguish from a first order jump. On the other hand an important difference from a true first order transition is that the latter shows hysteresis when driven at a finite rate whereas here hysteresis will be absent for  $\lambda < \lambda_c^*$  due to the fact that the surface energy is effectively negative. For  $\lambda > \lambda_c^*$  instead, hysteresis can appear.

Now we discuss the thermodynamic stability. In Fig. 1 we show the energy of the mixed state solutions. For finite  $\lambda$  the energy vs. density has a negative curvature in the mixed state indicating a negative electronic compressibility. For large  $\lambda$  the electronic compressibility in

the mixed state ( $|\bar{n} - n_c|/\delta n^0 < e^{-\pi\lambda^2}$ ) behaves as

$$\kappa_e^{-1} \sim -\frac{\kappa^{-1} e^{\pi\lambda^2}}{\sqrt{1 - [e^{\pi\lambda^2}(\bar{n} - n_c)/\delta n^0]^2}}. \quad (8)$$

$\kappa_e^{-1}$  negatively diverges at the uniform-mixed state transition and is exponentially large and negative for  $\bar{n} \sim n_c$ .

A negative divergence of the compressibility with a 1/2 critical exponent also arises at the uniform-stripe transition for small  $\lambda$  but with a strength that vanishes when  $\lambda \rightarrow 0$ .

In the present model the background is assumed to be incompressible ( $k_b = 0$ ) but real systems will have a small background compressibility  $k_b > 0$  and the system will become unstable when the total inverse compressibility  $k_b^{-1} + k_e^{-1} < 0$ . This will lead to a volume instability<sup>9</sup>, substituting the stripe transition with a volume collapse transition and reintroducing hysteresis<sup>28</sup>. This is the most likely behavior to be found in real systems specially for large  $\lambda$  where the electronic compressibility is large and negative in the whole mixed state stability range.

#### IV. 3D SYSTEMS

In this section we discuss the 3D case. The energy of a layered mixed state is given by Eq. (4) with  $D = 3$ , provided the effective interaction  $u(q)$  is given by

$$u(q) = (1 + l_s^2 q^2)^{-1},$$

and the screening length  $l_s$  is substituted by the usual 3D expression,

$$l_s = (4\pi Q^2 \kappa)^{-1/2}.$$

Notice that the standard 3D screened Coulomb interaction is given by  $u(q)/q^2$ .

The different nature of the screening in two- and three-dimensional systems affects strongly the properties of the mixed state. At the crossing density, the exact expression for the energy density of a layered state is minimized for  $\nu = R_d/R_c = 1/2$  and takes the following simple form:

$$e = \frac{\sigma}{R_c} \left[ 1 - \lambda^{-3/2} \tanh \frac{R_c}{2l_s} \right] \quad (9)$$

where  $\lambda$  is the 3D frustrating parameter:<sup>9</sup>

$$\lambda = 4 \left[ (\pi Q^2 \sigma^2) / (\kappa \Delta \mu_c^4) \right]^{1/3}.$$

The energy density of the uniform state is given by  $e = 0$ , hence for a layered state to be possible the term in the brackets in Eq. (9) must become negative. This condition is equivalent to the existence of a critical frustrating parameter  $\lambda_c = 1$  as it was derived in Ref. 9 within the UDA and now showed in an exactly solvable model.

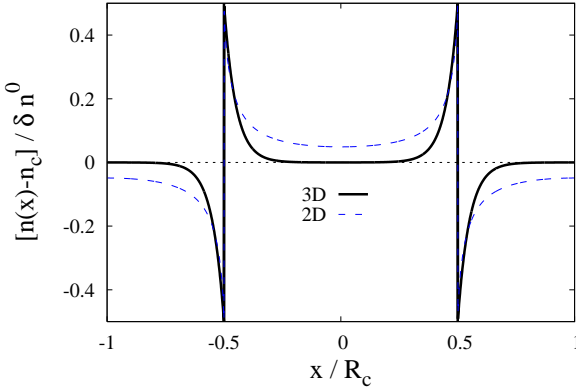


FIG. 7: (Color online) Charge density modulation for a cut perpendicular to the layers in 3D systems (thick line) and 2D systems (dashed line) at  $\bar{n} = n_c$  and a layer period  $R_c = 20l_s$ .

Minimizing Eq. (9) respect to  $R_c$  one finds that  $R_c$  is smaller than a few screening lengths except in the unphysical case in which  $\lambda$  is fine-tuned exponentially close to  $\lambda_c$ . This is in contrast with the 2D case where  $R_c$  is unbounded for a generic large  $\lambda$  (Fig. 6).

This result is due to the different screening effect in three-dimensions with respect to the 2D case. To illustrate this difference we plot in Fig. 7, the charge density in 2D and 3D in a cut perpendicular to the stripe/layer for  $R_c = 20l_s$ . In 3D the charge density decays exponentially from the interface over a distance of the order of the screening length whereas in 2D it decays as a power law. As emphasized in Ref. 9 the phase separation energy gain stems from the regions where the local density  $n(x)$  is significantly different from the global  $\bar{n}$  value. In 2D this is generically fulfilled and thus phase separation is favored. In 3D instead, the two densities are substantially different only in a region of width  $l_s$  around the interface. For  $\lambda < \lambda_c$  the phase separation energy gain from these regions compensates the surface and Coulomb energy cost and makes inhomogeneities possible. Instead the central region in the 3D case of Fig. 7 produces an exponentially small phase separation energy gain and therefore one never finds inhomogeneities with  $R_c >> l_s$ , as in the figure, unless  $\lambda$  is exponentially close to  $\lambda_c$ . Indeed one can check from Fig. 6 that this is the case for the present value of  $R_c/l_s$ .

The fact that strong variations of the density as the one pictured in Fig. 7 practically never occur in 3D makes the UDA reliable everywhere in the 3D phase diagram.

The exact 3D phase diagram for the layered state in the  $\lambda$ -density plane is shown in Fig. 8. As expected it is very similar to the one obtained within the UDA in Refs. 9,11. The only difference is that in the UDA the uniform-inhomogeneous transition resulted weakly first order whereas here it is second-order like due to a divergence of  $R_c/R_d$  as in 2D.

The main difference with the 2D case is that the two

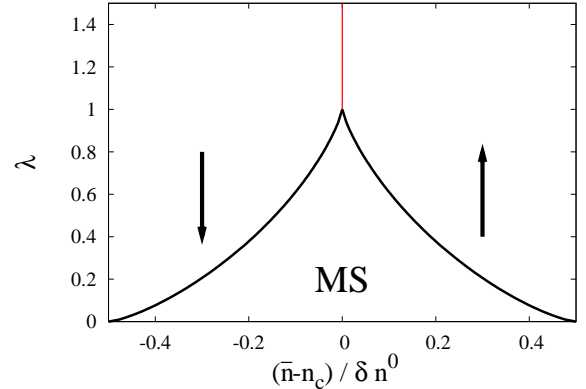


FIG. 8: (Color online) The phase diagram in the  $\lambda - (\bar{n} - n_c)/\delta n^0$  plane for three-dimensional systems. The thick lines correspond to the second-order transitions from the homogeneous phase to the smectic stripe phase characterized by a divergent periodicity and a finite minority phase layer size. The thin line represents the first order transition between the two homogeneous phases that occurs for  $\lambda > \lambda_c$ .

second order transition lines from the homogeneous phase to the mixed state touch each other at  $\lambda = \lambda_c$ . For  $\lambda > \lambda_c$  the systems has no intermediate state between the uniform phases and a direct first-order transition appears among them. In this case the energy density as a function of the global density is given by the lowest energy branch among the two parabolas shown in Fig. 1. This has a cusp singularity at  $n_c$  which produces a Dirac function like negative divergence of the compressibility. This leads to a volume instability also in this case<sup>9,28</sup>.

## V. CONCLUSIONS

In this work we have solved a model of phase separation frustrated by the LRC interaction while considering screening effects and the charge relaxation inside the domains in two and three dimensional systems.

In 2D and for high frustration the finite bare compressibility can be neglected. Its effect can be taken up by a short distance cutoff. In this regime, however, the mixed state requires very stringent conditions to be observed: *i*) it requires an enormously accurate control of the density since it appears in an exponentially narrow region around the crossing density, *ii*) the size of the domains grows exponentially with the frustration and may easily reach the size of the system, *iii*) the mixed state is characterized by an exponentially large negative compressibility which induces a volume instability when the rigidity of the background is not sufficient to stabilize the system altogether.

An incompressible background may seem unphysical according to the above discussion. However in some cases a sufficient separation of energy scales may avoid a volume instability if singularities in the compressibility are

rounded by extrinsic effects. For example in ruthanates and in the 2D electron gas the relevant electronic phenomena occurs at temperatures below a tenth of a Kelvin to be compared with melting temperatures of the material of the order of hundreds of Kelvin. Even when a volume instability may be avoided, the strongly frustrated mixed state may appear somewhat academic due to the stringent conditions on the density. An important physical, however, consequence is that the transition will look first order like but without hysteresis as discussed in Sec. III. In the case of the ruthanates there is the additional advantage that the control parameter is the magnetic field which allows for considerable fine-tuning.

For low frustration the finite bare compressibility of the phases [the third term in Eq. (1)] cannot be neglected. The mixed phase compressibility gets strongly renormalized. We have discussed its behavior in 2D [Eq. (8)] which in principle can be directly measured by capacitive techniques<sup>29</sup>. We have also shown that neglecting the spatial variation of the charge inside the domains, one obtains very accurate results at low frustration. From our results and Figs. 2,4 it is clear that the limit  $\kappa \rightarrow \infty$  and the UDA can be seen as the strong and the weak frustration approximation respectively for the full model Eq. (1).

In 3D systems the bare compressibility term is essential to obtain the mixed state with sharp interfaces as studied here and the UDA becomes reliable everywhere in the phase diagram.

The different role of the screening in 2D and 3D can be interpreted by noticing that the electronic charge density behavior inside the domains is dramatically different in 3D with respect to 2D. In the latter case, in fact, the charge density inside one stripe decays with a power-law from the interface and the local electronic charge density differs from the background density (i.e.  $n(\mathbf{x}) \neq \bar{n}$ ) over the entire stripe width. Thus domains gain phase separation energy in all the region and there is no limitation for their size. This also explains why the mixed state can appear independently on how strong the frustration is.

On the contrary, in 3D systems the charge density

decays exponentially. As a consequence, the system is forced to satisfy a “maximum size rule”<sup>9,11</sup> that states that for generic parameters the inhomogeneities cannot have all linear dimensions much larger than the 3D screening length  $l_s^{3D}$ . This allows for arbitrary large inhomogeneities in 2D since one of the dimensions is already smaller than  $l_s^{3D}$  as indeed found (Fig. 5).

The frustrating parameter can be written as

$$\lambda = \left[ 2^{D-1} \frac{l_d}{l_s} \right]^{1-\frac{1}{D}}$$

Here  $l_d$  represents the size that inhomogeneities should have for the surface energy cost,  $\sigma/l_d$ , be of the same order as the phase separation energy gain,  $e_0 = (\delta n^0)^2/\kappa$ .

To make a rough estimate of  $\lambda$  we go back to the lattice and take the bare compressibility as an inverse bandwidth  $\kappa = [2Dt]^{-1}$  with  $t$  an interatomic hopping integral. Defining a nearest neighbor Coulomb interaction  $V \equiv Q^2/a$  one obtains:

$$\begin{aligned} \lambda^2 &= \frac{\pi}{2} \frac{VJ}{t^2(\delta n_0)^2} & (D = 2) \\ \lambda^3 &= \frac{32\pi}{27} \frac{VJ^2}{t^3(\delta n_0)^4} & (D = 3) \end{aligned}$$

If one neglects the logarithmic singularity in 2D, inhomogeneities require  $\lambda \lesssim 1$ . In general we expect the scale  $J$  which may be due to magnetism or other low energy phenomena to satisfy  $J < t$ . According to our definitions  $\delta n_0$  is the difference of the Maxwell construction densities (measured as number of particles per site). Typically we expect weak phase separation tendency so  $\delta n_0 \ll 1$ . Comparing with the 2D case, the 3D case has an extra factor  $J/t$  that makes the mixed state more favorable and an extra factor  $\delta n_0^{-2}$  that makes the mixed state less favorable. A more precise analysis requires microscopic modeling of specific situations and will be presented elsewhere.

<sup>1</sup> C. Kittel, Phys. Rev. **70**, 965 (1946).

<sup>2</sup> E. L. Nagaev, *Physics of magnetic semiconductors* (MIR, Moscow, 1983).

<sup>3</sup> C. P. Lorenz, D. G. Ravenhall, and C. J. Pethick, Phys. Rev. Lett. **70**, 379 (1993).

<sup>4</sup> M. Seul and D. Andelman, Science **267**, 476 (1995).

<sup>5</sup> F. Sciortino, S. Mossa, E. Zaccarelli, and P. Tartaglia, Phys. Rev. Lett. **93**, 055701 (2004).

<sup>6</sup> E. L. Nagaev, A. I. Podel'shchikov, and V. E. Zil'bewarg, J. Phys.: Condens. Matter **10**, 9823 (1998).

<sup>7</sup> U. Löw, V. J. Emery, K. Fabricius, and S. A. Kivelson, Phys. Rev. Lett. **72**, 1918 (1994).

<sup>8</sup> C. Castellani, C. Di Castro, and M. Grilli, Phys. Rev. Lett. **75**, 4650 (1995).

<sup>9</sup> J. Lorenzana, C. Castellani, and C. Di Castro, Phys. Rev. B **64**, 235127 (2001).

<sup>10</sup> J. Lorenzana, C. Castellani, and C. Di Castro, Phys. Rev. B **64**, 235128 (2001).

<sup>11</sup> J. Lorenzana, C. Castellani, and C. Di Castro, Europhys. Lett. **57**, 704 (2002).

<sup>12</sup> C. B. Muratov, Phys. Rev. E **66**, 066108 (2002).

<sup>13</sup> R. Jamei, S. Kivelson, and B. Spivak, Phys. Rev. Lett. **94**, 056805 (2005).

<sup>14</sup> C. Ortix, J. Lorenzana, and C. Di Castro, Phys. Rev. B **73**, 245117 (2006).

<sup>15</sup> S. H. Pan, J. P. O'neal, R. L. Badzey, C. Chamon, H. Ding, J. R. Engelbrecht, Z. Wang, H. Eisaki, S. Uchida, A. K. Gupta, K.-W. Ng, E. W. Hudson, K. M. Lang, and J. C.

<sup>16</sup> Davis, *Nature (London)* **413**, 282 (2001).

<sup>16</sup> K. McElroy, R. W. Simmonds, J. E. Hoffman, D.-H. Lee, J. Orenstein, H. Eisaki, S. Uchida, and J. C. Davis, *Nature (London)* **422**, 592 (2003).

<sup>17</sup> K. M. Lang, V. Madhavan, J. E. Hoffman, E. W. Hudson, H. Eisaki, S. Uchida, and J. C. Davis, *Nature (London)* **415**, 412 (2002).

<sup>18</sup> R. A. Borzi, S. A. Grigera, J. Farrell, R. S. Perry, S. J. S. Lister, S. L. Lee, D. A. Tennant, Y. Maeno, and A. P. Mackenzie, *Science* **315**, 214 (2007).

<sup>19</sup> L. Zhang, C. Israel, A. Biswas, R. L. Greene, and A. de Lozanne, *Science* **298**, 805 (2002).

<sup>20</sup> M. P. Lilly, K. B. Cooper, J. P. Eisenstein, L. N. Pfeiffer, and K. W. West, *Phys. Rev. Lett.* **83**, 824 (1999).

<sup>21</sup> S. Ilani, A. Yacoby, D. Mahalu, and H. Shtrikman, *Science* **292**, 1354 (2001).

<sup>22</sup> C. Honerkamp, *Phys. Rev. B* **72**, 115103 (2005).

<sup>23</sup> S. A. Kivelson, E. Fradkin, and V. J. Emery, *Nature (London)* **393**, 550 (1998).

<sup>24</sup> P. M. Chaikin and T. C. Lubensky, *Principles of Condensed Matter Physics* (Cambridge University Press, Cambridge, 1995).

<sup>25</sup> E. Fradkin and S. A. Kivelson, *Phys. Rev. B* **59**, 8065 (1999).

<sup>26</sup> T. Ando, A.B.Fowler, and F.Stern, *Rev. Mod. Phys.* **54**, 437 (1982).

<sup>27</sup> The situation is reminiscent of the transition in a type II superconductor as a function of field at  $H_{c1}$ , which according to Ginzburg-Landau theory is second-order although normal state “drops” (the vortex core) have a finite radius  $\xi$ . See M. Tinkham, *Introduction to superconductivity* (McGraw-Hill, New York, 1975).

<sup>28</sup> S. Bustingorry, E. Jagla, and J. Lorenzana, *Acta Mater.* **53**, 5183 (2005).

<sup>29</sup> J. P. Eisenstein, L. N. Pfeiffer, and K. W. West, *Phys. Rev. B* **50**, 1760 (1994).